Effect of stiffness of protected secondary edge beams on the membrane behaviour of composite beam-slab systems in fire

Nguyen, Tuan-Trung; Tan, Kang-Hai

2014

Nguyen, T.-T., & Tan, K.-H. (2014). Effect of stiffness of protected secondary edge beams on the membrane behaviour of composite beam-slab systems in fire. 8th International Conference on Structures in Fire.

https://hdl.handle.net/10356/81424

8th International Conference on Structures in Fire
Shanghai, China, June 11-13, 2014

EFFECT OF STIFFNESS OF PROTECTED SECONDARY EDGE BEAMS ON THE MEMBRANE BEHAVIOUR OF COMPOSITE BEAM-SLAB SYSTEMS IN FIRE

Tuan-Trung Nguyen*, Kang-Hai Tan*

* Nanyang Technological Univ., School of Civil and Environmental Engineering, Singapore
e-mails: nguyentt@ntu.edu.sg, CKHTAN@ntu.edu.sg

Keywords: Tensile membrane action, Beam-slab systems, Composite slabs, Fire

Abstract. *This paper presents the experimental behaviour on two one-quarter scale composite beam-slab systems in fire. The aim was to study the effect of bending stiffness of protected secondary edge beams on the fire behaviour of floor assemblies. Two specimens were denoted as P215-M1099 and P486-M1099. To investigate the effect of second moment of area about the major axis of the protected secondary beam (I_{yPSB}), I_{yPSB} of P486-M1099 was increased 2.26 times compared to that of P215-M1099. The main and unprotected secondary beams of two specimens were kept the same. The test results showed that as the stiffness of the protected secondary edge beam increased, the slab deflection decreased and failure of the slab occurred later. However, composite action between the edge beams and the concrete slab played a key role in mobilising this beneficial effect. Once the composite action had been weakened by parallel cracks in the slab over the main or secondary edge beams, the slab would lose the benefit associated with the greater stiffness of the protected secondary edge beams.*

1 INTRODUCTION

From 2008 till recently, there has been a surge of interest on the membrane behaviour of integrated composite slab-beam floor systems in fire [1-5]. These studies offer valuable insight into the fire behaviour of composite slab-beam systems. However, there is no experimental work investigating the influence of stiffness of protected edge beams on the fire behaviour of the floor assemblies. When the protected edge beams deform under fire conditions, the boundary condition of the composite slab changes and this has significant effect on the development of tensile membrane action (TMA). In literature, there was only a numerical study to address this problem. Lim [6] conducted a parametric study to investigate the slab behaviour with different edge beam sizes. He concluded that as the beam size decreases, failure of the slab occurs earlier with a much greater slab deflection. Although the positive effect of the beam size on the slab behaviour was confirmed by the numerical study, important effects such as concrete cracking and local damages were not taken into account.

To bridge this technical gap, a series of tests including six one-quarter composite beam-slab floor systems in total have been conducted at Nanyang Technological University, Singapore in 2012. A gamut of stiffness ratios for the protected edge beams has been investigated ranging from 1.0 to 2.26 for the protected secondary edge beams and 1.00 to 1.92 for the protected main edge beams. This is so far the only experimental programme studying the effect of stiffness of protected edge beams on the development of TMA. The series to study the effect of the protected secondary edge beams included three specimens, namely, P215-M1099, P368-M1099 and P486-M1099, in which their corresponding stiffness ratios were 1.00, 1.71 and 2.26, respectively. This paper presents only the experimental behaviour of two specimens, P215-M1099 and P486-M1099. The aim was to study the effect of *bending stiffness of protected secondary edge beams* on the fire behaviour of floor assemblies.

2 TEST SPECIMENS AND SETUP

2.1 Test specimens

Numerical studies [7] showed that in terms of the four geometric properties of the protected edge beams (steel grade, torsional rigidity GI_t, bending stiffness about the major axis EI_y, bending stiffness about the minor axis EI_z), only the bending stiffness about the major axis EI_y has significant effect on the membrane behaviour of floor assemblies. Therefore, the bending stiffness about the major axis EI_y was chosen as the main parameter.

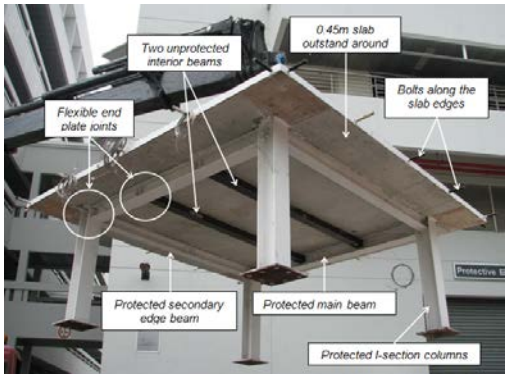

Figure 1. Typical specimen

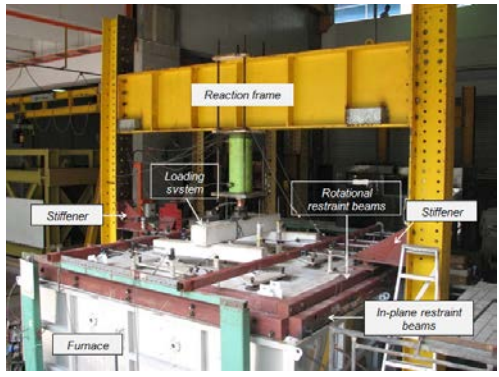

Figure 2. Test setup

Two specimens were denoted as P215-M1099 and P486-M1099. In this nomenclature, P215-M1099 indicates a specimen which has 215cm^4 as the second moment of area about the major axis of protected secondary edge beam (I_{yPSB}), and 1099cm^4 as that of main edge beam (I_{yMB}). Specimen P215-M1099 was chosen as the control specimen. I_{yPSB} of P486-M1099 was increased 2.26 times compared to that of P215-M1099. The protected main and unprotected interior secondary beams for these specimens were kept the same. The effect of two unprotected interior beams on tensile membrane behaviour of beam-slab systems has been investigated separately [8].

Figure 1 shows a typical specimen with the slab 2.25m long by 2.25m wide and an outstand of 0.45m around the four edges. The dimensions of the specimens were limited by those of the electric furnace. Therefore, the slab dimensions were scaled down by ¼ from a prototype floor which was designed for gravity loading in accordance with BS EN 1994-1-1. Along each edge were five M24 bolts with half of these bolt lengths cast into the slab, while the other half were attached to the in-plane restraint system as described in Section 2.2. The locations of these bolts were fixed by using 8mm thick steel plates along the four slab edges. The purpose of these bolts was to simulate accurately the boundary conditions of interior slab panels. The interior slab panels should be rotationally restrained and could only have horizontal straight movement along the four edges.

It is of interest to find out if the slab edges would translate straight if the slab is considered as an interior slab. Considering a composite steel-framed building, the common fire scenario is the situation where the fire heats up the whole soffit of the floor. In this situation, the displacement along the slab edges can be outward caused by thermal expansion, or inward resulted from tensile membrane action mobilised at a later stage. However, the common edges between two interior slab panels must translate straight to ensure displacement compatibility. Therefore, in this case the slab edges can only displace outwards and inwards maintaining a straight edge. This experiment focused on this fire scenario.

The concrete slab thickness was 57mm and 55mm for P215-M1099 and P486-M1099, respectively. Shrinkage reinforcement mesh with a grid size of 80mm x 80mm and a diameter of 3mm (giving a reinforcement ratio of 0.16%) was placed within the slab, 25mm from the top. The mesh was continuous

across the whole slab with a yield strength of 689MPa. The specimens were cast using ready-mixed concrete with aggregate size ranging from 5 to 10mm. Six concrete cylinders were tested at 28 days giving a characteristic cylinder strength f_{ck} of 31.3MPa and 28.9MPa for P215-M1099 and P486-M1099, respectively.

Material and geometrical properties of the I-section steel beams are given in Table 1. The beams were designed for full-shear composite action using 40 mm long, 13 mm diameter headed shear studs with a spacing of 80mm so that no unexpected failure occurred due to shear. A common type of steel joints, i.e. flexible end plates, was used for beam-to-beam and beam-to-column connections.

Table 1 Details of steel beams

Specimen	*Denote*	*Depth*	*Width*	*Web thick. (mm)*	*Flange thick. (mm)*	*Yield strength (MPa)*	*Ultimate strength (MPa)*	*Elastic modulus (GPa)*
P215-M1099	MB1	131	128	7.0	11.0	307	462	211.4
	PSB1	**80**	**80**	10.3	10.0	467	588	210.6
	USB	80	80	10.3	10.0	467	588	210.6
P486-M1099	MB1	131	128	7.0	11.0	307	462	211.4
	PSB3	**102**	**101**	7.2	8.7	356	510	205.4
	USB	80	80	10.3	10.0	467	588	210.6

This experiment applied the fire protection strategy for members recommended in the SCI Publication P288 [9]. All the edge beams and columns were protected to a prescriptive fire-protection rating of 60min. No fire-proofing material was applied to the interior beams and the slabs.

2.2 Test setup

An electric furnace of dimensions 3m long by 3m wide by 0.75m high was setup at Nanyang Technological University. The dimensions of the furnace were dictated by the space constraint of the fire laboratory. Although the furnace could not simulate the ISO 834 fire curve, from the trial tests the furnace air temperature could attain 1000^{o}C within 50 minutes (min), i.e. at a heating rate of about 20^{o}C/min, which was within the practical heating rate for steel sections as prescribed in BS 5950-8.

The specimens were setup together with two restraint beam systems as shown in Figure 2. *The first system* was the rotational restraint system which consisted of four 160x100x6 rectangular hollow section (RHS) beams placed on top of these specimens and fixed to the reaction frame via two triangular stiffeners. It is assumed that reinforcement continuity over the supporting protected edge beams and the 0.45m slab outstand provided very little rotational restraint, since there was only one layer of shrinkage reinforcement inside the slabs.

The second system was the 'so-called' in-plane restraint system, which also consisted of four 160x100x6 RHS beams. This system was fixed to four slab edges via five M24 bolts along each edge at a spacing of 750mm (Figure 1). The in-plane restraint system was also connected to the rotational restraint system by a different line of bolts. These two systems aimed to simulate accurately the boundary conditions of interior slab panels. The in-plane restraint system allowed the slab edges to translate inwards or outwards in straight edges, while the rotational restraint system applied flexural restraint on the slab edges. Test results presented in Section 3 indicate that this research purpose has been achieved. It is worth noting that there was a 20mm gap between the in-plane restraint system and the furnace walls to avoid any load taken up by the furnace walls. The gap was filled by insulation material to avoid heat loss.

2.3 Instrumentation

K-type thermocouples and linear variable differential transducers (LVDT) were used to measure temperatures and displacements of the beams and the slab. A similar set of instrumentation was used for the two specimens. Temperature of the slab was measured at Sections 1, 2 and 3 (Figure 3). At each section, temperature was monitored at the top and bottom surfaces, and at the level containing the

reinforcing mesh. Temperatures of the beams were measured at Sections A to F at the top and bottom flanges, and at the middle of the beam web. The furnace air temperature was also monitored.

A total of 20 LVDTs were used to measure displacements of the floor assemblies (Figure 4), in which L1 to L3 were 300mm LVDTs to monitor vertical deflection of the slab. L4 to L11 comprised 200mm LVDTs to measure vertical deflections of the beams. Three 50mm LVDTs (L12, L13 and L14) were used to measure horizontal and vertical displacements of a column, while L15 to L20 for horizontal displacements along the slab edges.

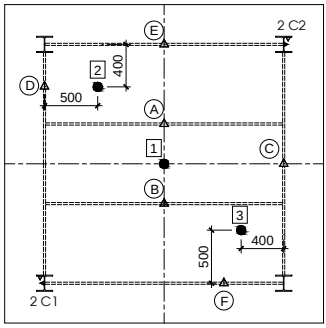

Figure 3. Arrangement of thermocouples

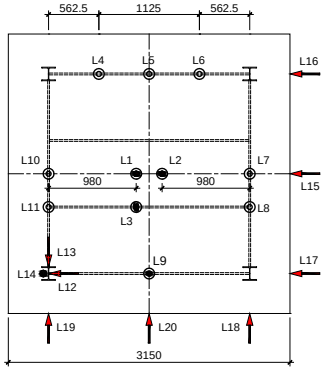

Figure 4. Arrangement of LVDTs

2.4 Test load

The slabs were initially loaded up to 15.8kN/m^2 by a twelve-point loading system designed to simulate uniformly distributed loads (Figure 2) and then heated up to failure from the soffit of the slab. This value was equal to 0.35 times of the conventional yield-line load at ambient temperature, which was 45.1kN/m^2 based on the slab configuration with two interior beams. The moment capacity of supporting beams does not affect the conventional yield-line load since it was assumed that the slab was "simply-supported" all round. The selection of load ratio is within the practical range of 0.3 to 0.7.

3 EXPERIMENTAL RESULTS AND DISCUSSIONS

3.1 Temperature distributions in the slabs

A comparison of distribution of slab temperatures of P215-M1099 and P486-M1099 is shown in Figure 5. It can be observed that the air temperature developed consistently in both tests. A small discrepancy of 5.8% was found when comparing the temperature at 94min of heating, viz. 966^{o}C in P215-M1099 against 910^{o}C in P486-M1099. On the other hand, temperature at the slab bottom surface increased at the same rate up to 60min of heating. After that, as the temperature increased gradually concrete cracks developed resulting in significant heat loss. Therefore, towards the end of the tests, the temperature at the bottom surface and at the reinforcing mesh showed some discrepancies. Temperature at the top surface was very consistent with the maximum value of 164^{o}C in P486-M1099.

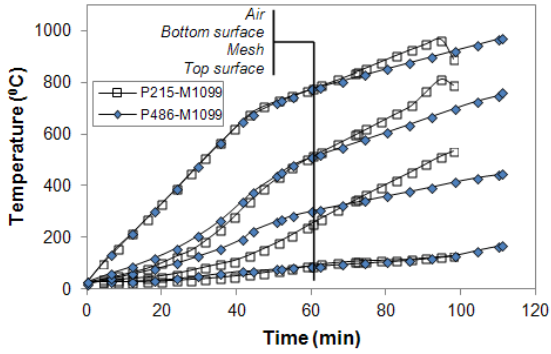

Figure 5. Distribution of slab temperatures

3.2 Slab displacements

3.2.1 Deflection at the slab centre

Deflection at the centre of P215-M1099 and P486-M1099 against the mesh temperature is plotted in Figure 6. It should be noted that the bending stiffness about the major axis of PSB (EI_{yPSB}) of P486-M1099 had increased 2.26 times compared to that of control specimen P215-M1099.

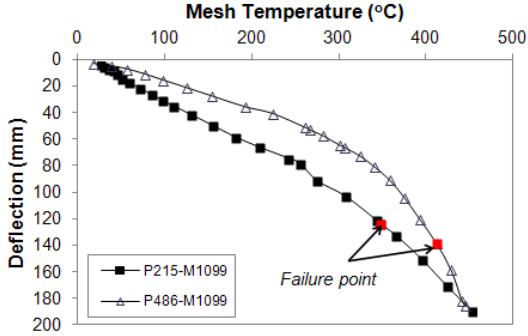

Figure 6. Comparison of deflection at the slab centre

P215-M1099 failed at a deflection of 124mm when the mesh temperature had reached 348°C. The corresponding values were 139mm at 412°C for P486-M1099. It can be observed that as the stiffness of PSB increased, the slab deflection decreased.

Table 2 Summary of test results

Specimen	h_s	*Failure time after fire*	*Failure temperature* (°C)*			p_{test}	$p_{y,\theta m}$	w_{max}	w_{max} / h_s	p_{test} / $p_{y,\theta m}$
	mm	*min*	θ_t	θ_m	θ_b	*kN/m²*	*kN/m²*	*mm*		
P215-M1099	57	72.2	108	348	602	15.6	8.4	124	2.17	1.86
P486-M1099	55	98.2	127	412	697	15.5	8.2	139	2.53	1.89

*θ_t: temperature at slab top surface; θ_m: temperature at reinforcing mesh; θ_b: temperature at slab bottom surface; h_s: slab thickness; $p_{y,\theta m}$: yield line load at failure mesh temperature.

With regard to the maximum deflection at failure, as can be seen in Table 2, P486-M1099 (EI_{yPSB} of P486-M1099 increased 2.26 times compared to that of P215-M0119) experienced a larger deflection, i.e. $2.53h_s$ compared to $2.17h_s$ for P215-M1099 (h_s is the slab thickness), which was an increase of 17%. However, the enhancement factor of P486-M1099 was only slightly greater than that of P215-M1099, 1.89 for P486-M1099 compared to 1.86 for P215-M1099. The enhancement factor is defined here as the ratio between the test load p_{test} and the yield line load at failure mesh temperature $p_{y,\theta m}$. This means that stiffness of the edge beams had little effect on tensile membrane stage of the slab. This was because at tensile membrane stage, the composite action between the edge beams and the concrete slab was weakened by parallel cracks appearing along the protected edge beams as shown in Section 3.4.

Therefore, it can be concluded that an increase of the stiffness of protected secondary edge beams had a positive effect on minimising the slab deflection. However, the composite action between the edge beams and the concrete slab plays a key role in mobilising this beneficial effect. Once the composite action was weakened by parallel cracks along the protected secondary beams, the floor system would lose the benefit associated with a greater stiffness of secondary edge beams.

3.2.1 Horizontal displacement

Figures 7 and 8 show the horizontal displacements of P215-M1099 and P486-M1099 respectively, including the loading phase. In these figures, a positive value indicates inward horizontal displacement, and a negative value outward displacement. The positions of the LVDTs are shown in Figure 4. L15, L16, L17 were placed along the edge parallel to the main beam, while L18, L19, L20 were placed parallel to the secondary edge beam. Three important observations can be drawn from these test results.

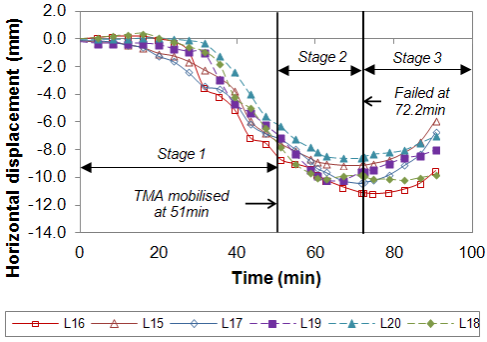

Figure 7. Horizontal displacement of the slab edges vs. time – P215-M1099

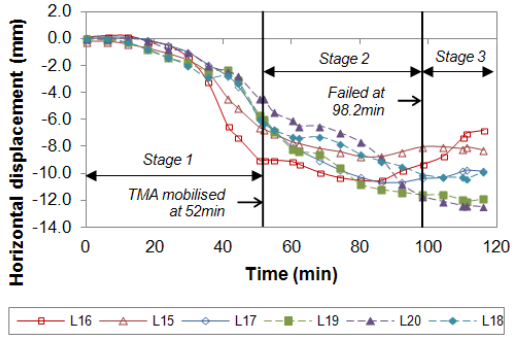

Figure 8. Horizontal displacement of the slab edges vs. time – P486-M1099

Firstly, the horizontal displacement-time relationship of the slabs can be divided into three stages. *In the first stage*, the slab edges moved outwards due to thermal expansion as the slab temperature increased. Up to 20min of heating, the temperature was low because the moisture in the slab had gradually released. Therefore, displacements of the edges in two horizontal directions were small, only about 2mm. From 20min to about 50min of heating, the displacements increased at a greater rate with the maximum values of 8mm and 9mm for P215-M1099 and P486-M1099, respectively. *In the second stage*, after 50min, when the slab deflection reached about $1h_s$, TMA was mobilised. Therefore, the sum of outward displacements due to thermal expansion and inward displacement due to TMA resulted in an almost constant displacement. *In the third stage*, when the slab experienced large vertical deflections, the slab edges moved inwards significantly. However, intense tensile stresses in the reinforcement above the protected edge beams led to failure in these regions. When the failure had been identified, the furnace was turned off.

Secondly, the onset of TMA can be marked based on the horizontal displacement-time relationship of the slabs. This was the time when the displacement rate reduced and was almost constant. As explained above, this resulted from the sum of outward displacement due to thermal expansion and inward displacement due to TMA. Therefore, TMA was mobilised at 51min and 52min for P215-M1099 and P486-M1099, respectively. These times are confirmed once again by the development of crack patterns in the slabs (Section 3.3).

Thirdly, it can be observed that the recorded horizontal displacements from L15, L16 and L17 along one slab edge and those from L18, L19 and L20 along the transverse slab edge were only slightly different. This indicates that the slab edges initially moved outwards and then inwards in straight lines. Therefore, it can be concluded that the tested slab panels could accurately simulate the continuity conditions of interior panels as initially planned.

3.3 Development of crack patterns

The development of crack patterns of P215-M1099 and P486-M1099 was observed carefully during the tests and is re-plotted in Figures. 9 and 10, respectively. The heating times when cracks occurred are indicated, together with the corresponding temperatures in the reinforcing mesh and the corresponding mid-span slab deflections. The crack sequences shown by the numbers were quite consistent in all the tests.

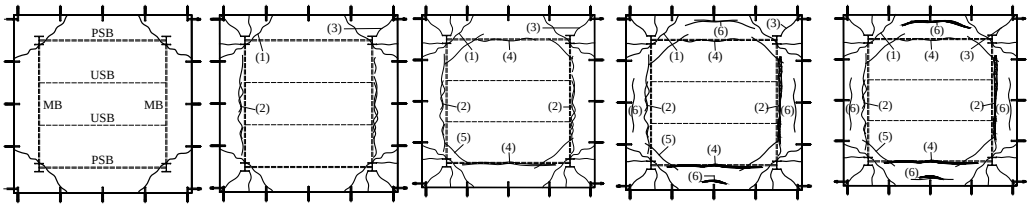

13min – 41°C 9mm | 33min – 91°C 28mm | 51min – 181°C* 59mm ≈ 1.03h_s | 72min – 348°C** 124mm | 87min – 458°C 178mm

Figure 9. Development of crack pattern – P215-M1099

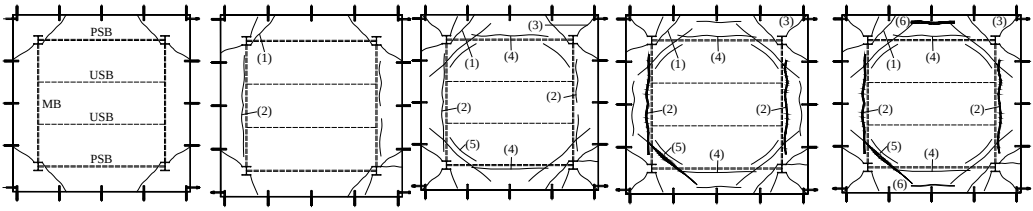

12min – 41°C 7mm | 31min – 79°C 15mm | 52min – 185°C * 54mm ≈ 0.98h_s | 98min – 412°C** 139mm | 110min – 496°C 182mm

Figure 10. Development of crack pattern – P486-M1099

Firstly, diagonal cracks near the beam-to-column joints (crack 1) appeared consecutively at the four slab corners. These cracks were due to biaxial bending of the slab outstand. At these corners, parts of the outstand were in biaxial bending but restrained by the columns.

Secondly, cracks appeared in the vicinity of the main beams (crack 2). The diagonal cracks emanating from the slab corners to the columns (crack 3) were then observed. These diagonal cracks (3) were caused by the bolts which restrained the slab. As the temperature increased, cracks along the protected secondary edge beams (crack 4) appeared.

In P215-M1099 test, after 51min of heating, a compression ring began to form when the mesh temperature had reached 181°C at a deflection of 59mm, 1.03h_s (h_s is the slab thickness). In P486-

M1099, a compression ring began to form at the respective mesh temperature of 185^{o}C, after 52min of heating at a mid-centre deflection of 54mm, equal to 0.98h_s. Based on this observation, it can be concluded that TMA mobilised at a slab deflection approximately equal to 0.9 to 1.0 of the slab thickness, irrespective of the stiffness of the protected edge beams. Tensile membrane mechanism in these tests consisted of radial tension in the central area of the slab, surrounded by a peripheral compression ring. Due to its self-equilibrating nature, horizontal edge restraint was not required for the mobilisation of TMA.

The onset of TMA can be recognised by appearances of diagonal cracks inside the slab panel at the four corners (crack 5). The more obvious indication was the transition between outward and inward displacements of the slab edges (Section 3.2.1). These indications coincided very well in terms of time.

Severe cracks also appeared at the slab outstand (crack 6). These cracks were due to the bolts along the slab edges. As the slab deflected, these bolts were too stiff to deflect together with the slab causing the cracks near the ends of the bolts. When the slab experienced very large deflections, the cracks opened through the slab thickness and reinforcement was fractured. However, this did not affect the test results because it happened after the failure had been identified.

3.4 Failure modes

The failure mode observed in P215-M1099 and P486-M1099 was fracture of reinforcement close to the protected edge beams (at crack 2 or 4). No run-away failure was observed. Shear studs and connections were shown to be designed adequately. No premature failure at the shear studs or at the connections was observed. Figures 11 and 12 show the final failure mode of P215-M1099 and P486-M1099 after cooling, respectively, in which the crack positions were indicated.

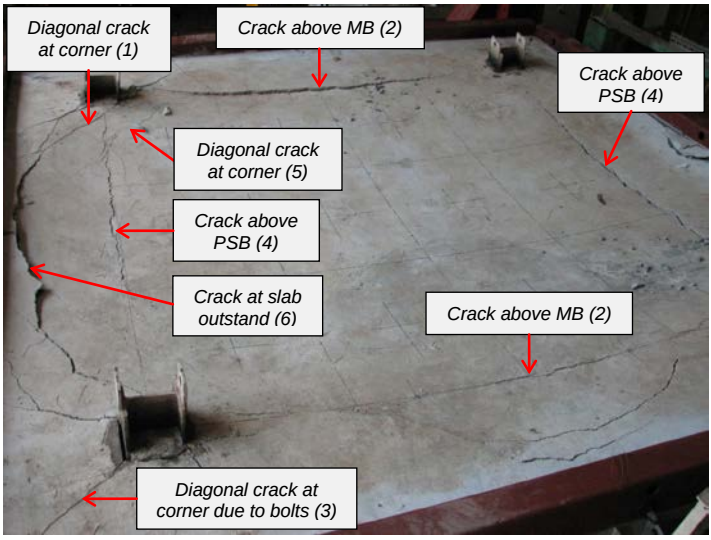

Figure 11. Failure mode of P215-M1099

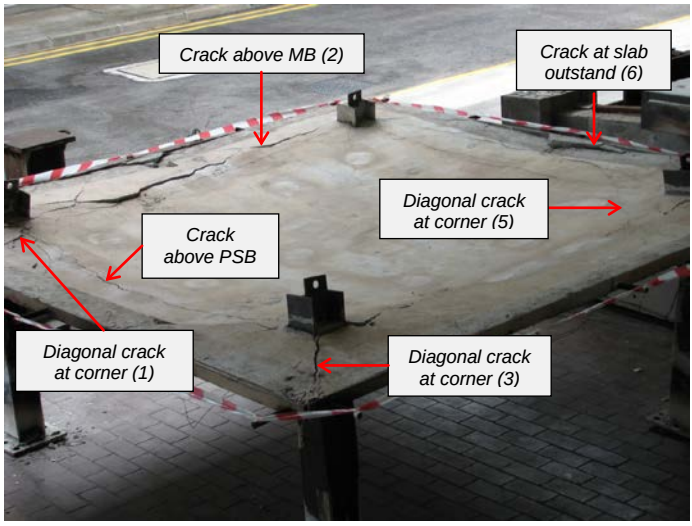

Figure 12. Failure mode of P486-M1099

4 CONCLUSIONS

This paper presents the experimental results and observation from two composite beam-slab floor systems tested under fire conditions. The aim is to study the effect of *bending stiffness of protected secondary edge beams* on the tensile membrane behaviour of floor assemblies in fire.

The results showed that as the stiffness of the protected secondary edge beams increased, the slab deflection initially decreased. However, composite action between the edge beams and the concrete slab plays a key role in mobilising this beneficial effect. Once the composite action had bean weakened by parallel cracks in the slab over the main or secondary protected edge beams, the benefit associated with a greater stiffness of the edge beams was lost.

Tensile membrane action was mobilised at a deflection equal to 0.9 to 1.0 of the slab thickness, irrespective of the bending stiffness of the edge beams. The occurrence of tensile membrane stage was marked by one of two indications: (a) concrete cracks which formed a peripheral compressive ring on top of the slabs, and (b) horizontal displacements along the slab edges. In both the tests, these indications were very consistent in terms of occurrence time.

ACKNOWLEDGMENT

The research presented in this paper was funded by Agency for Science, Technology and Research (A*Star Singapore) under Grant No. M4070013. The financial support of A*Star is gratefully acknowledged.

REFERENCES

[1] Zhao B., Roosefid M., and Vassart O. "Full scale test of a steel and concrete composite floor exposed to ISO fire", *Proceedings of the Fifth International Conference on Structures in Fire (SiF'08)*. Singapore, Nanyang Technological University, 539-550, 2008.

[2] Zhang N.-S., Li G.-Q., Lou G.-B., Jiang S.-C., and Hao K.-C. "Experimental study on full scale composite floor slabs under fire condition", *Application of Structural Fire Engineering*. Prague, Czech Republic502-511, 2009.

[3] Stadler M., Mensinger M., Schaumann P., and Sothmann J. "Munich Fire Tests on Membrane Action of Composite Slabs in Fire - Test Results and Recent Findings", *Application of Structural Fire Engineering*. Prague, Czech Republic2011.

[4] Ward F. and Kallerová P. "Fire Test on Administrative Building", *7th International Conference on Steel & Aluminium Structures*. Kuching, Sarawak, Malaysia2011.

[5] Wellman E., Varma A., Fike R., and Kodur V., "Experimental Evaluation of Thin Composite Floor Assemblies under Fire Loading", *J Struct Eng - ASCE*, (Vol 137, N0. 9), 1002-1012, 2011.

[6] Lim L.C.S. *Membrane action in fire exposed concrete floor systems*. Ph.D. Thesis. Department of Civil Engineering. University of Canterbury. 2003.

[7] Nguyen T.-T. *Behaviour of Composite Beam-Slab Floor Systems at Elevated Temperatures.* Ph.D. Thesis. School of Civil and Environmental Engineering. Nanyang Technological University. 2014.

[8] Nguyen T.T. and Tan K.H. "Testing of Composite Slab-beam Systems at Elevated Temperatures", *7th International Conference on Structures in Fire (SiF)*. 6-8 June 2012 Zurich, Switzerland, Swiss Federal Institute of Technology Zurich, 247-256, 2012.

[9] Newman G.M., Robinson J.T., and Bailey C.G., *Fire Safe Design: A new Approach to Multi-Story Steel-Framed Buildings*, in *SCI Publication P288* 2006, The Steel Construction Institute.